Measuring shape complexity of breast lesions on ultrasound images

Wei Yang[a], Su Zhang*[a], Yazhu Chen[a]
Wenying Li[b], Yaqing Chen[b]
[a]Dept. of Biomedical Engineering, Shanghai Jiao Tong Univ., Shanghai, China, 200240;
[b]Shanghai Sixth People's Hospital, Shanghai Jiao Tong Univ., Shanghai, China, 200231

ABSTRACT

The shapes of malignant breast tumors are more complex than the benign lesions due to their nature of infiltration into surrounding tissues. We investigated the efficacy of shape features and presented a method using polygon shape complexity to improve the discrimination of benign and malignant breast lesions on ultrasound. First, 63 lesions (32 benign and 31 malignant) were segmented by K-way normalized cut with the priori rules on the ultrasound images. Then, the shape measures were computed from the automatically extracted lesion contours. A polygon shape complexity measure (SCM) was introduced to characterize the complexity of breast lesion contour, which was calculated from the polygonal model of lesion contour. Three new statistical parameters were derived from the local integral invariant signatures to quantify the local property of the lesion contour. Receiver operating characteristic (ROC) analysis was carried on to evaluate the performance of each individual shape feature. SCM outperformed the other shape measures, the area under ROC curve (AUC) of SCM was 0.91, and the sensitivity of SCM could reach 0.97 with the specificity 0.66. The measures of shape feature and margin feature were combined in a linear discriminant classifier. The resubstitution and leave-one-out AUC of the linear discriminant classifier were 0.94 and 0.92, respectively. The distinguishing ability of SCM showed that it could be a useful index for the clinical diagnosis and computer-aided diagnosis to reduce the number of unnecessary biopsies.

Keywords: breast cancer, image segmentation, shape analysis, feature extraction

1. INTRODUCTION

Breast ultrasound is a useful adjunct to X-ray mammography in reducing the number of negative biopsy results. The clinical analysis of breast images is currently almost exclusively done by a qualitative assessment of lesion features within an image[1]. In the clinical evaluation of breast lesions on ultrasound, radiologists consider features that include lesion shape, margin definition, echogenic texture, posterior acoustic enhancement, or shadowing[2]. The interpretation of ultrasound images, however, is highly dependent on the experience and subjectiveness of radiologists who review and analyze the features of the lesion. Variations in human perception of the images, differences in features used for diagnosis, and, more fundamentally, a lack of quantitative measurements of the features used for image analysis are some of the factors that cause variability in diagnosis by individuals. Consequently, the final confirmation of benign or malignant diagnosis usually requires a biopsy. Computerized schemes have been proposed to reduce this operator dependency and to provide a more objective interpretation of ultrasound findings. The effective computer-aided diagnosis (CAD) system had been shown to improve the diagnostic accuracy of radiologists in the task of distinguishing between malignant and benign breast lesions and in avoiding unnecessary biopsy[3].

The potential of sonographic texture analysis to improve breast tumor diagnosis has already been demonstrated[4-7]. However, the texture is dependent on the imaging equipments and settings. Malignant breast tumors and benign lesions have different shape characteristics: the former usually are rough, spiculated, or microlobulated, whereas the latter commonly are smooth, round, oval, or macrolobulated. Joo et al.[8] used the polar coordinates of boundary pixels of nodule images with the origin at their center of mass to obtain numeric values representing this feature, were calculated. However, the polar coordinates of boundary pixels can not represent effectively the shape of tumor since that it is possible that two points with the same angle have different radial distance. Chou et al.[9] used the statistical parameters

* suzhang@sjtu.edu.cn; phone +86-21-34205825.

Medical Imaging 2008: Ultrasonic Imaging and Signal Processing, edited by Stephen A. McAleavey, Jan D'hooge, Proc. of SPIE Vol. 6920, 69200J, (2008) · 1605-7422/08/$18 · doi: 10.1117/12.770959

derived from the radial length of boundaries to classify the breast tumors. Chen et al.[10] proposed five morphologic features for breast CAD, which were nearly setting independent and could tolerate reasonable variation in boundary delineation. Kim et al.[11] evaluated the shape features of breast masses using a computerized scheme and to correlate the feature values with radiologists' grading. Objective shape features, such as compactness, fractal dimension, elliptic-normalized circumference[10], elliptic-normalized skeleton[10], convex hull depth[11], etc. have been used to distinguish benign masses from malignant tumors using pattern recognition methods for computer- aided diagnosis of breast cancer on ultrasound images. Actually, more similar objective shape measures, such as fractional concavity[12], spiculation index[12], index of convexity from turning angle function[13], Fourier- descriptor-based factor[14], etc. have been also developed to distinguish benign masses from malignant tumors for CAD of breast cancer on mammography. All these shape measures represent quantitatively shape complexity of beast tumors in some degrees.

The purpose of our study is to find the effective shape measures which can characterize the shape complexity of the breast tumors. First, the breast tumors are segmented by K-way normalized cut[15-16] with the proposed empirical rules. Then, the polygonal model and the local integral invariant signature are used to represent the lesion contours. We introduce a shape complexity measure (SCM) of polygon[17] to the breast ultrasound, which quantified directly the shape complexity and was proposed primarily for query processing and optimization in spatial databases[17]. The distinguishing ability of SCM is compared to the other shape measures[18]. Finally, the performance of a linear classifier using the shape complexity and the measures of margin feature as the input vector is evaluated.

2. METHODOLOGY

2.1 Segmentation of breast lesions on ultrasound images by K-way normalized cut

Notwithstanding the relative success of shape measures in the classification of breast tumors, completely automatic contour extraction on the ultrasound image remains to be a difficult problem. There some efforts and wonderful approaches on this issue[8, 19-21]. Considering the fact that the breast radiologists can locate easily the suspicious lesion region which covers only small portion of each original image, we start with the manually segmented region of interest (ROI) of the lesion. Rectangular ROI of the lesion area is first segmented out manually. The segmentation of images to separate the lesion from the surrounding tissues is performed by means of the filter based on total variation minimization and oscillatory functions[22] and K-way normalized cut (Ncut) algorithm[16].

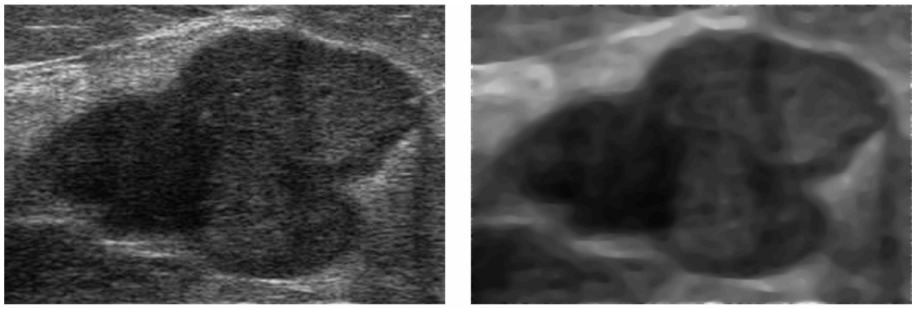

(a) (b)

Fig. 1. The original ROI of a malignant tumor (a) and the corresponding cartoon image (b).

Due to the noise and speckles in the ultrasound images, first, some noise filtering methods are needed to reduce the noise. And then, the segmentation method will work more efficiently. The speckle noise can be treated as the texture and decomposed from the ultrasound image by the variational model which combined the total variation minimization model with spaces of oscillatory functions[22]. Then the cartoon image after the decomposition process is segmented. Compared to the original image, the noise on the cartoon image is removed efficiently and the detailed structures are not lost. Actually, Nuct can easier segment the lesion region on this kind of cartoon images than the images filtered by others filter techniques such as median filtering and anisotropic diffusion in the experiments. Fig.1 shows an original ultrasound image and the corresponding cartoon image.

Normalized cut proposed by Shi and Malik[15] formulates segmentation as a graph-partitioning problem. It maximizes the total dissimilarity between the different groups and the total similarity within the groups. This segmentation technique readily admits combinations of different features such as brightness, position, windowed histograms, etc., and has been successfully used in object parsing and grouping on the natural and medical images[21, 23]. Normalized cut had been developed to the multiclass spectral clustering method– K-way Ncut[16].

To apply the K-way Ncut to segment the cartoon image, the parameter K must be set beforehand. The different K would result in the different segmentations. Ncut was employed to partition an image into many small regions until the object function of Ncut reached its minimum, and then the adjacent regions were merged into several bigger regions[21]. We found that the over-segmentation could be avoided and the merging process was not necessary if K was appropriate. The value of K was suggested to set as the number of the tissue type on MRI image[23]. But the number of tissue type is ambiguous in the ultrasound images. As shown in Fig.2, the possible number of tissue type is 2 or 3. Actually, we can not obtain the ideal segmentation with K=2 or K=3.

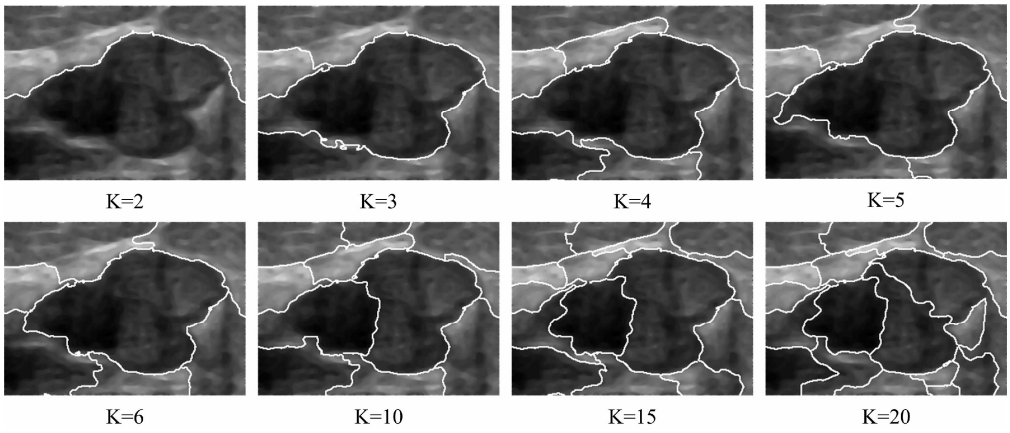

Fig. 2. The segmentation results of the cartoon image with incremental K.

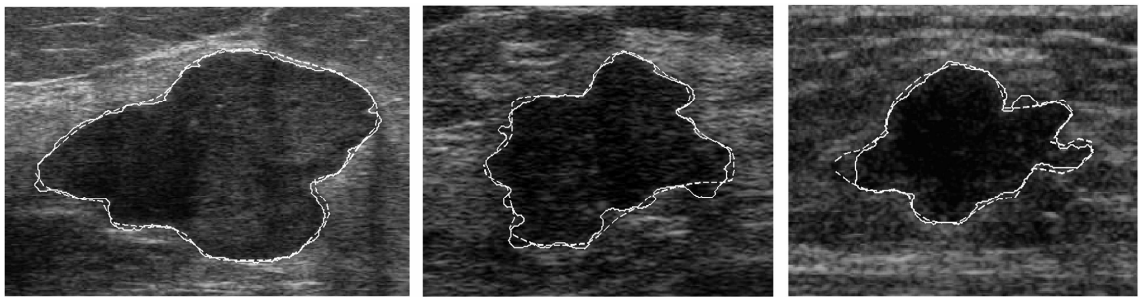

Fig. 3. The lesion contours extracted by K-way Ncut and the physician. The solid lines are the automatically extracted contours. The dashed lines are the manual contours.

K-way Ncut produced a pseudo-hierarchical segmentation as shown in Fig.2: when K increased, regions tended to be successively divided, yet the enclosing boundaries were subject to fine adjustment. The image would be over-segmented if K was too large (e.g. K=15) and the lesion region could not be merged from the small regions. There is no common rule to determine the optimal K. We choose K through the following empirical rules based on that the lesion region is darker than its surrounding tissue and the centroid of lesion is located approximately at the center of ROI[18].

1. The lesion region which is closest to the center of ROI is isolated to the margin of ROI with certain *k*.
2. Set *k*'=*k*+1 and segment the image with *k*' if *k* satisfies rule1. The optimal K is selected as *k*' if the overlap area of the lesion regions corresponding to *k*' and *k* is larger than 95% of the lesion area corresponding to *k*. This rule

ensures that the lesion region corresponding to *k* is not under-segmented and the lesion region corresponding to *k*' is not over-segmented.

3. The segmentation process is failed if there is no *k* satisfies rule1 and rule2.

K ranged from 2 to 8. For the case in Fig. 2, the selected K is 6. To improve the computing efficiency, the multiscale, graph decomposition[24] algorithm for K-way Ncut was implemented in the segmentation stage. Fig. 3 shows the segmentation results by K-way Ncut with the proposed empirical rules. The global shapes of segmented lesions are rather similar to the manual ones. Furthermore, K-way Ncut can capture more structural details of lesion contours than human.

2.2 Shape analysis of lesion contour

In this paper, we adopted local integral invariant (LII) signatures[25-27] and polygonal approximation to represent the contour.

2.2.1 Polygonal approximation of lesion contour and shape complexity measure

The initial contours extracted from the segmented lesions are usually jagged and sensitive to noise, which have too many vertices. Polygonal approximation is required not only to reduce the amount of data to be processed subsequently, but also to preserve most of the shape information of the initial contours. It is a convenient representation for shape analysis and recognition, and its perimeter can also be calculated efficiently. In recent decades, a number of methods have been proposed for polygonal approximation. Since dominant points represent a local shape property and allow their efficient representation for applying feature extraction, we employ a modified polygonalisation algorithm based on adaptive dominant point detection[28] to obtain the polygonal represent of the tumor contour. The aim of polygonalisation in this paper is to obtain the compact represent of digitized contour and preserve the structures of spicules and lobes along the tumor contour.

The adaptive dominant point detection method proposed by Wu[28] is used to detect the dominant points, which computes the suitable length of support region for each point to find the best approximated curvature and the dominant points are identified as the points with local maximum curvatures. In addition, the break point detection is conducted to reduce the computations. The detected dominant points with a given threshold of curvature (set to -0.8 in the experiments) are not suitable polygonal represent for the breast tumor contour. There may be too many vertices or too few vertices to fit the contour. The merging and splitting schemes similar to[12, 26] are iteratively implemented until convergence using the dominant points as the initial polygonal vertices. In the merging scheme, the line segments with length less than the threshold (set to 3 pixels in the experiments) are merged to one of its adjacent line segments so that the smaller integrated squared error (ISE) can be obtained, and the two adjacent line segments with the angle greater than a given threshold (set to 170°) are merged to one line segment. In the splitting scheme, the arc-to-chord distance is computed for all the vertices and the point on the contour with the maximum arc-to-chord deviation greater than the threshold (set to 5 pixels) is located as a new polygonal vertices. Contrast to the algorithm in[12, 29], the adaptive dominant point detection can reduce significantly the number of irrelevant points and avoid estimating the curvatures with a fixed scale. The final results of polygonal models of the boundaries of two malignant tumors are shown in Fig.4.

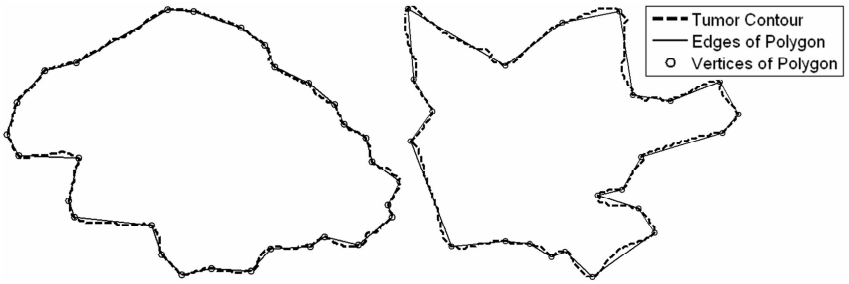

Fig. 4. The polygonal models of two malignant tumor contours.

We introduce a shape complexity measure of polygon proposed by[17] to characterize the complexity of contour. The complexity of a polygon *pol* is defined as follows:

$$\mathrm{SCM}(pol) = w_1 \times ampl(pol) \times freq(pol) + w_2 \times conv(pol),$$

where w_1 and w_2 are the weight coefficients, $ampl(pol)$ and $freq(pol)$ are the amplitude and frequency of the vibration of the polygon, $conv(pol)$ is the global shape convexity measure. The weight coefficients w_1 and w_2 are set to 0.9 and 0.1, respectively. $freq(pol)$ is computed as follows:

$$freq(pol) = 16(normnotche(pol) - 0.5)^4 - 8(normnotche(pol) - 0.5)^2 + 1,$$

where *normnotches* is the normalized number of notches. Notches describe the non-convex parts of a polygon, which are the vertices of the polygon with the interior angle larger than π. Let *notches* and *vertices* describe the number of vertices and the number of notches, respectively. The number of notches can be normalized to the interval [0, 1] by

$$normnotche(pol) = notches(pol) / (vertices - 3),$$

since the following property holds:

$$notches(pol) \le vertices - 3,$$

The polygons show the highest vibration when *normnotches* is about 0.5 and the lowest vibration for values of 0 and 1.

ampl(pol) is defined as the relative increase of the boundary compared to its convex hull:

$$ampl(pol) = (boundary(pol) - boundary(convexhull(pol))) / boundary(pol),$$

where *boundary*() indicates the operator to compute the perimeter of polygon, *convexhull*(*pol*) indicates the convex hull of polygon. If the polygon is convex, *ampl* will be 0. The higher the amplitude is, the longer the boundary is and the higher *ampl* is. 1 is the unreachable limit of *ampl*.

conv(*pol*) is the convexity of a polygon with the following formula:

$$conv(pol) = (area(convexhull(pol)) - area(pol)) / area(convexhull(pol)).$$

A convex polygon has a very simple shape, whereas a polygon which strongly differs from its convex hull is considered to have a complex shape. *conv* is 0 for a convex polygon. The higher the deviation of the polygon from its convex hull, the higher *conv* is.

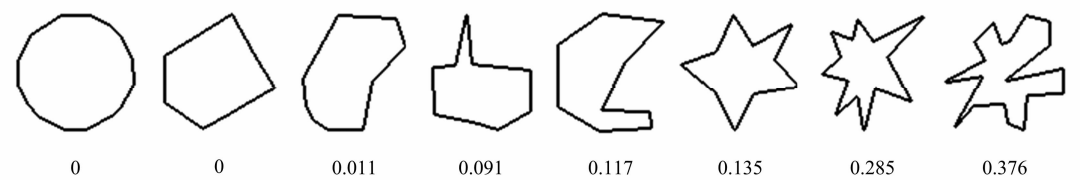

Fig. 5. The synthetical polygons and the values of their SCM.

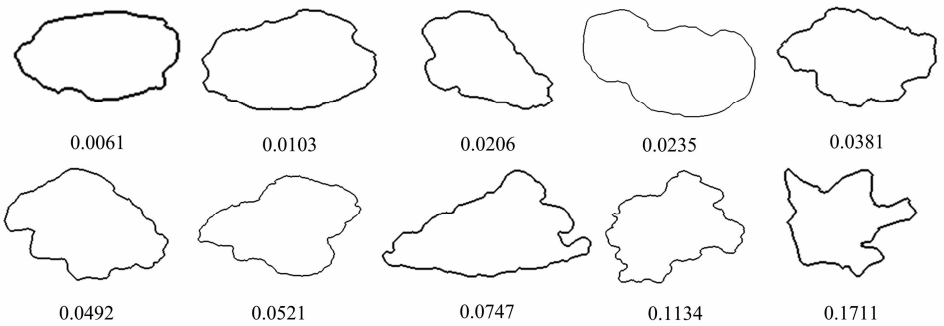

Fig. 6. The automatic extracted tumor contours and the values of their SCM.

SCM is in the range [0, 1]. The rough, spiculated, or microlobulated contours lead to the complex polygons whereas the smooth, round, oval, or macrolobulated contours lead to the simple convex polygons. Fig. 5 shows the synthetical shapes and the values of their shape complexity. It can be clearly seen from Fig. 5 that the results are in accordance with the perception of humans. Fig. 6 shows the segmented lesion contours and the values of their complexity measures. From Fig 6, the more lobes and spicules occur on the lesion contour, the larger value of SCM is. The values of SCM close to 0 indicate a simple contour and values larger than 0.05 occur for the contours with the lobes and sipcules.

2.2.2 Local integral invariant signatures

The local integral invariant is an effective descriptor for shape and a local change of a shape affects the values of the integral invariant for the entire shape, which have been applied to shape matching successfully. In general, the term feature F_σ indicates any image statistic. In particular, local features are functions of the image defined on a compact subset of its domain, including 'soft' versions where the 'effective subset' is determined by a kernel[25]:

$$F_\delta(\chi, x) = K_\delta * \chi(x),$$

where K_σ is a Gaussian kernel: $K_\delta(x) = e^{-\|x\|^2/2\delta^2}/(\sqrt{2\pi}\delta)$.

Applied to a binary image χ, the feature value F_σ computed at a boundary point is related to the curvature at that point with a given scale σ[25, 27]. From (1), F_σ is bounded between 0 and 1. In fact, F_σ entails a regularized notion of curvature in a scale-space even where the boundary is not differentiable[25]. In[25, 27] F_σ was called as local area integral invariant. F_σ is robust to noise (lack of differentiability) of the boundary. As defined in the feature function, a scale is associated with features of interest and various levels of features can be characterized in a feature scale-space with varying scales. Despite the fact that local features entail 'blurring' with a kernel, the geometrical shape attributes are precisely preserved in the shape representation[26]. Fig.7 shows a tumor contour and its LII signatures.

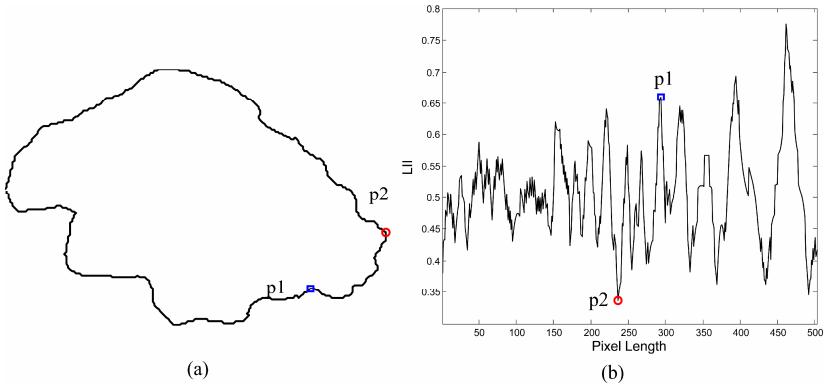

Fig. 7. A contour of segmented malignant tumor (a) and the corresponding LII signatures (b).

Three new measures are derived from the local integral invariant signatures to quantify the local anfractuosity of lesion contours. The standard deviation (SD) of LII:

$$SD = \sqrt{\sum_{i=1}^{N} (F_\delta(i) - F_{\delta Avg})^2 / (N-1)},$$

where $F_{\sigma Avg}$ is the mean of F_σ and N is the number of boundary pixels.

The entropy of LII:

$$Entropy = -\sum_{k=1}^{nbins} p_k \log(p_k),$$

where p_k is the probability that the value of LII is between (k-1)/$nbins$ and k/$nbins$, p_k is computed via a normalized histogram, and $nbins$ is set to 32.

The roughness index of contour:

$$Roughness = \log(\sum_{i=1}^{N} \left| F_\delta(i+n) - F_\delta(i) \right| / N),$$

where n is the interval of boundary points.

2.2.3 Other shape measures

There are many others useful shape measures proposed by the researchers for distinguishing the malignant and benign lesions. Spiculation can be particularly valuable, since it provides a direct radiographic manifestation of the local aggressivity of invasive breast cancer. Some spiculation measures were proposed by the researchers, such as spiculation index (SI)[12], fractional concavity (Fcc) [12], and index of convexity (CI_{TA}) from the turning angle function[13]. SI[12] is a measure derived by combining the ratio of the length to the base width of each possible spicule in the contour of the given lesion and is computed from the polygonal model. CI_{TA}[13] is derived from the smoothed turning angle function. Fractional concavity (Fcc) is a measure of the portion of the indented length to the total contour length; it is computed by taking the cumulative length of the concave segments and dividing it by the total length of the contour[12]. Others shape descriptors, such as Depth–Width Ratio (DWR), Compactness, Irregularity, Solidity, Convex Hull Depth (CHD)[11], Elliptic-Normalized Circumference (ENC)[10], Elliptic-Normalized Skeleton (ENS) [10], Fourier Factor (FF) [14], box-counting Fractal Dimension (FD) [13] are also computed from the lesion contours extracted automatically by K-way normalized cut.

3. RESULTS

3.1 Images data

The ultrasound image database comprises 63 images of pathologically proven benign breast lesions from 32 patients and carcinomas from 31 patients. The images were collected from 2003 to 2006; the patients' ages ranged from 18 to 75 years. Sonography was performed using two types of scanners with the 7.5-15 MHz linear transducers. The database was supplied by the coauthor, an experienced physician, Dr. Chen, from the Shanghai Sixth People's Hospital, Shanghai.

3.2 Segmentation results

For each ROI, the lesion contour was extracted using K-way Ncut. Three cases with heavy shadowing and calcification failed in the segmentation stage and had been corrected manually. The mean of match rate between the manually determined lesion region and the automatically detected region was 88% and the mean of Hausdorff distance between their contours was 15.5 pixels which were estimated using 10 ROI with the manual contours. The performance of the proposed segmentation method was compared to some reported methods[18, 19-21].

3.3 Performance of shape complexity measure

To evaluate the performance of each individual shape feature, a receiver operating characteristic (ROC) curve was generated by using a sliding threshold on each feature and computing the sensitivity and specificity for each threshold. The true-positive fraction (TPF), or sensitivity, is the proportion of the malignant cases correctly identified by the classifier. The false-positive fraction (FPF) is the proportion of the benign cases incorrectly identified by the classifier as malignant. The TPF and the FPF are plotted to yield the ROC curve. The overall classification performance is summarized by the area under the ROC curve (AUC).

When we use local integral invariant to characterize the lesion contour, the effect of scale parameter σ should be considered. The experimental results suggested that 12 pixels is the appropriate value for σ. Tab.1 lists AUC of the all 16 shape measures. The results from Table 1 show that SCM has the best performance (AUC=0.913). The distribution of SCM is shown in Fig.8. In Fig.8, the benign and malignant classes are clearly separated. The mean of SCM on the

benign and malignant cases are 0.0261 and 0.0852, respectively. Fig.9 shows the ROC curve of SCM. The sensitivity of SCM can reach 0.97 with the specificity 0.66.

Table 1. AUC of the shape measures

Measure	SCM	SD of LII	Entropy of LII	RI	SI	CI_{TA}	Fcc	FF
AUC	**0.913**	0.864	0.862	0.796	0.773	0.772	0.687	0.832
Measure	ENC	ENS	Irregularity	CHD	Compactness	Solidity	FD	DWR
AUC	0.880	0.822	0.545	0.883	0.830	0.883	0.755	0.665

3.4 Classification using linear discriminant analysis

Atypical cases of macrolobulated or spiculated benign lesions, as well as microlobulated or well-circumscribed malignant tumors create difficulties in pattern classification. It is difficult to distinguish completely the benign and malignant lesions only using the shape features. Actually, radiologists consider features that include lesion shape, margin definition, echogenic texture, posterior acoustic enhancement, or shadowing in the clinical evaluation of breast lesions on ultrasound. Since the texture measures vary nonlinearly with the system settings, we only extract four measures of margin feature which are relatively independent of the imaging settings. The extracted measures of margin features are Normalized Radial Gradient Index[30], Relative Brightness[31] and Margin sharpness[32]. The selected measures of shape features are SCM, Entropy of LII, and Elliptic-Normalized Circumference.

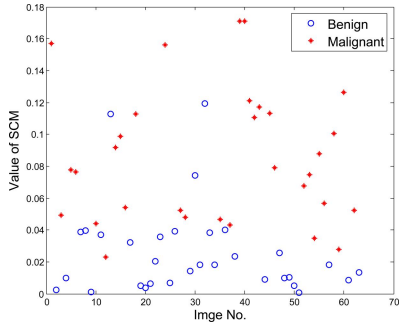

Fig.8. The distribution of SCM.

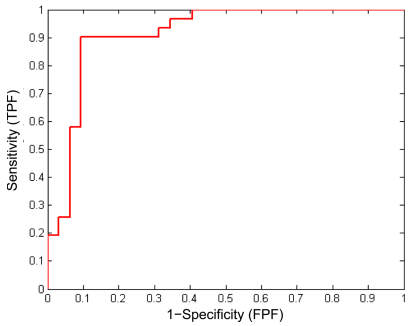

Fig.9. ROC curve of SCM.

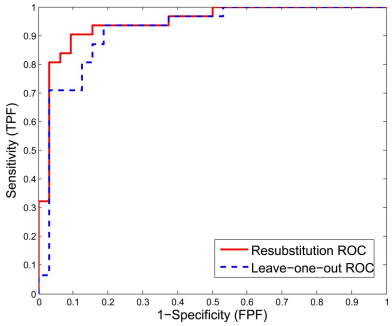

Fig.10. ROC curves of LDA classifier.

There are various classification methods which can be used to build the classifier for the breast tumor CAD. Since the amount of image samples is limited, to avoid the over-optimistic estimation, we used linear discriminant analysis (LDA) to merge the computer-extracted features. ROC analysis was also used to evaluate the performance of LDA classifier in the task of distinguishing benign from malignant lesions. We used two techniques to estimate the ROC: the resubstitution method, which has an optimistic bias (estimated higher than the actual), and the leave-one-out method, which has a pessimistic bias. In resubstitution, the same set of cases is used for training (computing classifier parameters) as for testing (estimating the ROC). In a leave-one-out analysis a subset of all but one case is used for training, then the classifier output, is computed for the case that was taken out. This is repeated for all cases, generating a table of statistics that are used for ROC analysis. The ROC curves of LDA classifier are shown in Fig. 10. The resubstitution and leave-one-out AUC are 0.943 and 0.916, respectively.

4. DISCUSSION AND CONCLUSIONS

This paper introduced a new measure of shape complexity to characterize the automatic extracted tumor contours, which outperformed the other measures of shape features. Compared to the terminologies about shape in the BI-RADS lexicon[33] for ultrasonography including ‘Oval’, ‘Round’, and ‘Irregular’, SCM is an objective, continuous index and will be not ambiguous in the computerized scheme. The significant difference of SCM between the benign and malignant lesions suggested that it would be a useful index for the clinical diagnosis to reduce the number of unnecessary biopsies.

Combining SCM, Entropy of LII, and the margin features, a simple LDA classifier had the classification performance compared to the various proposed CAD models. More effective classifier methods, such as support vector machine and boosting, can also be used to build the classifier for the CAD system. However, the current image database only contained a limited amount of ultrasound images. We used LDA to obtain the consistent estimation of classification performance. The AUC of the proposed system is up to 0.92.

However, the conclusions of this paper are limited by the size of the study samples. The proposed system only used measures of shape and margin features. The methods to extract effective measures which can quantity echo pattern, surrounding tissue, and calcifications should be developed. In the nearly future, we will collect more breast ultrasound images and develop the classification system on ultrasound for pathology types of breast lesion.

ACKNOWLEDGMENTS

This work is supported by National Basic Research Program of China (973 Program) (No. 2003CB716103), Project of Shanghai Science and Technology Committee (No. 064119632), and NSFC (No. 60573033).

REFERENCES

[1] M.S. Chandra, P.W. Susan, H.A. Peter, F.C. Emily, "A review of breast ultrasound," J. Mammary Gland Biol. Neoplasia. **11**, 113-123 (2006).

[2] A.T. Stavros, D. Thickman, C.L. Rapp, M.A. Dennis, S.H. Parker, G.A. Sisney, "Solid breast nodules: use of sonography to distinguish between benign and malignant lesions," Radiology **26(1)**, 123-134 (1995).

[3] K. Horsch, M.L. Giger, C.J. Vyborny, L.A. Venta, "Performance of computer-aided diagnosis in the interpretation of lesions on breast sonography," Acad. Radiol. **11**, 272-28 (2004).

[4] Y.L. Huang, K.L. Wang, D.R. Chen, "Diagnosis of breast tumors with ultrasonic texture analysis using support vector machines," Neural Comput. Applic. **15(2)**, 164-169 (2006).

[5] R. Sivaramakrishnaa, K.A. Powella, M.L. Lieberb, W.A. Chilcotec, R. Shekhara, "Texture analysis of lesions in breast ultrasound images," Comput. Med. Imaging Graph. **26**, 303-307 (2002).

[6] S.J. Chen, K. Cheng, Y.C. Dai, et al. "Quantitatively characterizing the textural features of sonographic images for breast cancer with histopathologic correlation," J. Ultrasound Med. **24(5)**, 651-661 (2005).

[7] N. Piliouras, I. Kalatzis, N. Dimitropoulos, D. Cavouras, "Development of the cubic least squares mapping linear-kernel support vector machine classifier for improving the characterization of breast lesions on ultrasound," Comput. Med. Imaging Graph. **28(5)**, 247-55 (2004).

[8] S.Y. Joo, Y.S. Yang, W.K. Moon, H.C. Kim, "Computer-aided diagnosis of solid breast nodules: use of an artificial neural network based on multiple sonographic features," IEEE Trans. Med. Imaging **23(10)**, 1292-1300 (2004).

[9] Y.H. Chou, C.M. Tiu, G.S. Hung, S.C. Wu, T.Y. Chang, H.K. Chiang, "Stepwise logistic regression analysis of tumor contour features for breast ultrasound diagnosis," Ultrasound Med. Biol. **27**, 1493–1498 (2001).

[10] C.M. Chen, Y.H. Chou, K.C. Han, G.S. Hung, C.M. Tiu, H.J. Chiou, S.Y. Chiou, "Breast lesions on sonograms: computer-aided diagnosis with nearly setting-independent features and artificial neural networks," Radiology **226**,504-514 (2003).

[11] K.G. Kim, S.Y. Cho, S.J. Min, J.H. Kim, B.G. Min, K.T. Bae, "Computerized scheme for assessing ultrasonographic features of breast masses," Acad. Radiol. **12**, 58-66 (2005).

[12] R.M. Rangayyan, N.R. Mudigonda, J.E.L. Desautels, "Boundary modeling and shape analysis methods for classification of mammographic masses," Med. Biol. Eng. Comput. **38**, 487-496 (2000).

[13] D. Guliato, J.D. Carvalho, R.M. Rangayyan, S.A. Santiago, "Feature extraction from a signature based on the turning angle function for the classification of breast tumors," J. Digital Imaging, published online (2007).

[14] S. Liang, R.M. Rangayyan, J.E.L. Desautels, "Application of shape analysis to mammographic calcifications," IEEE Trans. Med. Imaging **13(2)**, 263-274 (1994).

[15] J. Shi and J. Malik, "Normalized cuts and image segmentation," IEEE Trans. Pattern Anal. Mach. Intell. **22(8)**, 888-905 (2001).

[16] S.X. Yu and J. Shi, "Multiclass spectral clustering," IEEE Int. Conf. on Computer Vision (ICCV'2003), 313-319 (2003).
[17] T. Brinkhoff, H.P. Kriegel, R. Schneider, A. Braun, "Measuring the complexity of polygonal objects," Proc. ACM Int. Workshop on Advances in Geographic Information Systems, 109-117 (1995).
[18] S. Zhang, W. Yang, H.T. Lu, Y.Z. Chen, W.Y. Li, YQ Chen, "Automatic feature extraction and analysis on breast ultrasound images," Communications in Computer and Information Science **(2)**, 957-963 (2007)
[19] A. Madabhushi and D.N. Metaxas, "Combining low-, high-Level and empirical and domain knowledge for automated segmentation of ultrasonic breast lesions," IEEE Trans. Med. Imaging **22(2)**, 155-169 (2003).
[20] T.W. Cary, E.F. Conant, P.H. Arger, C.M. Sehgal, "Diffuse boundary extraction of breast masses on ultrasound by leak plugging," Med. Phys. **32(11)**, 3318-3328 (2005).
[21] X. Liu, Z.M. Huo, J.W. Zhang, "Automated segmentation of breast lesions in ultrasound images," Proc. IEEE Eng. Med. Biol. 27th Annual Conf., 7433-7435, Shanghai, China (2005).
[22] L.A. Vese and S.J. Osher, "Image denoising and decomposition with total variation minimization and ascillatory functions," J. Mathematical Imaging and Vision **20**, 7-18 (2004).
[23] J. Carballido-Gamio, S. J. Belongie, S. Majumdar, "Normalized cuts in 3-D for spinal MRI segmentation," IEEE Trans. Med. Imaging **23(1)**, 36–44 (2004).
[24] T. Cour, F.Benezit, J. Shi, "Spectral segmentation with multiscale graph decomposition," Proc. IEEE Conf. on Computer Vision and Pattern Recognition (CVPR'05) **2**, 1124-1131 (2005).
[25] S. Manay, B. Hong, A. Yezzi, S. Soatto, "Integral invariant signatures," Lecture Notes in Computer Science **2034**, 87-99 (2004).
[26] B.W. Hong, E. Prados, L. Vese, S. Soatto, "Shape representation based on integral kernels: application to image matching and segmentation," Proc. IEEE Conf. on Computer Vision and Pattern Recognition (CVPR'06), 833-840 (2006).
[27] S. Manay, D. Cremers, B.W. Hong, Jr.A.Yezzi, S. Soatto, "Integral invariants for shape matching," IEEE Trans. Pattern Anal. Mach. Intell. **28(10)**, 602-1618 (2006).
[28] W.Y. Wu, "An adaptive method for detecting dominant points," Pattern Recognition **(36)**, 2231-2237 (2003).
[29] D. Guliato, R.M. Rangayyan, J.D. Carvalho, S.A. Santiago, "Spiculation-preserving polygonal modeling of contours of breast tumors," Proc. 28th Annual Int. Conf. IEEE Eng. in Med. and Biol. Society (EMBS'2006), 2791-2794, New York (2006).
[30] K. Horsch, M.L. Giger, L.A.Venta, C.J. Vyborny, "Computerized diagnosis of breast lesions on ultrasound," Med. Phys. **29**, 157-164 (2002).
[31] M. Ito, T. Chono, M. Sekiguchi, T. Shiina, H. Mori, E. Tohno, "Quantitative evaluation of diagnostic information around the contours in ultrasound images," J. Med. Ultrasonics **32**, 135-144 (2005).
[32] C.M. Sehgal, T.W. Cary, S.A. Kangas, S.P. Weinstein, S.M. Schultz, P.H. Arger, E.F. Conant, "Computer-based margin analysis of breast sonography for differentiating malignant and benign masses," J. Ultrasound Med. **23**: 1201-1209 (2004).
[33] L. Elizabeth, B.M. Martha, S. Barbara, L.K. Susan, S.L. Linda, "BI-RADS lexicon for US and mammography: interobserver variability and positive predictive value," Radiology **239**, 385-391 (2006).